

Frame Synchronization Method Based on Association Rules for CNAV-2 Messages

LI Xinhao, MA Tao, and QIAN Qishu

(National University of Defense Technology, Hefei 230037, China)

Abstract — The GPS system is a navigation satellite system with high precision, all-weather service, and global coverage, whose main purpose is to provide real-time and continuous global navigation services for the US military, and whose signal interference in wartime is a heavy blow to the US military. Its existing interference measures are classified into two types: blanket jamming and deception jamming, with the latter having better interference effects due to its imperceptibility. Frame synchronization, as the foundation of deception jamming, is a focus of current research on navigation countermeasures. This paper discusses the frame synchronization of CNAV-2 messages in GPS L1C signals and proposes a frame synchronization algorithm based on association rules. It analyzes the structural characteristics of CNAV-1 message data, reveals the hidden mapping relationships in the BCH code sequence of the first sub-frame by applying association rules, and achieves a blind synchronization of navigation messages by counting the types of mapping relationships and calculating the confidence levels. The simulation test results show that the proposed algorithm displays high error resilience and correct recognition rates and demonstrates certain values in engineering applications.

Key words — CNAV-2 message, Frame synchronization, Association rule, Confidence level.

I. Introduction

With ever-increasing requirements of navigation applications in both military and civilian uses, upgraded measures have been adopted in the United States in recent years in order to modernize the global positioning system (GPS). For civilian signals, L1C signals are introduced to the L1 frequency band of the GPS system [1]–[4]. The L1C signals are composed of data signals and pilot signals. In the data signals, navigation messages and pseudo-codes are modulated, and

the signal power is estimated to be 25% of the total power. In the pilot signals, overlay codes and main codes are modulated, and the signal power is estimated to be 75% of the total power [5]. Due to the greater share of the pilot signals in terms of signal power, a significant increase in the code error rate of the received data signals is observed. In order to solve this problem, error correction codes are introduced, and a frame structure without a fixed synchronization header is adopted for CNAV-2 messages in the L1C data signals, which creates new challenges for the frame synchronization of CNAV-2 messages [6], [7]. Therefore, it is of great significance to conduct research on an effective frame synchronization method for navigation messages targeted at CNAV-2 messages.

In the relevant literature, there is limited research on the frame synchronization of CNAV-2 messages. In [8], a frame synchronization method based on correlation computation and coherent accumulation is proposed to address the shortcomings of existing frame synchronization methods related to subcodes, such as long synchronization time and high computational complexity. In this method, sub-code chips with a fixed length are generated; correlation computation and coherent accumulation are performed for the above chips and the received sub-codes with the same length, and the calculation results are compared with the detector thresholds in order to examine the synchronization accuracy. Although the shortcomings of the sub-code-related synchronization methods are overcome, the synchronization results are significantly affected by the detector thresholds, and frame synchronization cannot be achieved under high code error rates. In [9], a sliding window method is adopted for frame synchronization considering the fact that the overlay codes in the L1C

pilot signals have the same length as the navigation message frames. In this method, the overlay codes with a fixed length are modulated to build the sliding window; this window is slid across the entire cycle of the local overlay codes, and the correlation value is obtained by correlation computation, and the sliding distance is obtained for the correlation peak to achieve frame synchronization. However, considering the fact that the cycle time of the local overlay codes is 18 seconds, a long synchronization time is observed, and synchronization accuracy cannot be maintained under high code error rates. In [10], beginning with the shift registers which generate synchronized code of CNAV-2 message, this paper designs a fast adaptive synchronization algorithm. In this synchronization algorithm, the first step is estimating the number of error bit in the front nine bit of 52 bit, an integral BCH coding. Then, filter and sort these possible pairs of sequences. When the maximum correlation in the two adjacent frames are counted, frame synchronization is implemented. However, synchronization accuracy cannot be maintained under high code error rates.

In this paper, an association rule-based frame synchronization method for navigation messages is proposed, which provides a new way of thinking about frame synchronization. By configuring the value of minimum support, the number of candidate item-sets was greatly reduced, improving the computational efficiency of the proposed algorithm. On the basis of type analysis of mapping relations and value determination of confidence level, the proposed algorithm was found to

outperform the existing algorithm in terms of error performance.

II. CNAV-2 Messages

In the L1C data signals, the CNAV-2 original message data $D_{L1C}(t)$ is coded into CNAV-2 message data coding symbols $d_{L1C}(t)$ after modulation. The messages are provided with a frame structure. For each frame, the transmission time is estimated as 18 seconds, and a total of 1800 data coding symbols are recorded. In other words, the symbol rate is 100 sps; and for each symbol, the code width is 10 ms [6].

1. Message structure and coding

In each frame, the CNAV-2 original message data $D_{L1C}(t)$ is composed of three sub-frames with different lengths. The first sub-frame is composed of 9-bit time of interval (TOI) data; the second sub-frame is composed of the 576-bit original message data code and the 24-bit cyclic redundancy check (CRC) code, and the third sub-frame is composed of the 250-bit original message data code and the 24-bit CRC code.

In CNAV-2 messages, BCH coding is adopted for the first sub-frame, whereas subframes 2 and 3 of the CNAV-2 messages are encoded first with a 24-bit CRC parity algorithm, and then with a Low Density Parity Check (LDPC) code in order to obtain 1200-bit and 548-bit coding symbol data. Then, these code sequences are arranged to form a 1748-bit data string. Finally, the interleaved coding is adopted for this string in order to obtain 1748-bit information, as shown in Fig.1.

2. Message structure analysis

The coded CNAV-2 message data is composed of

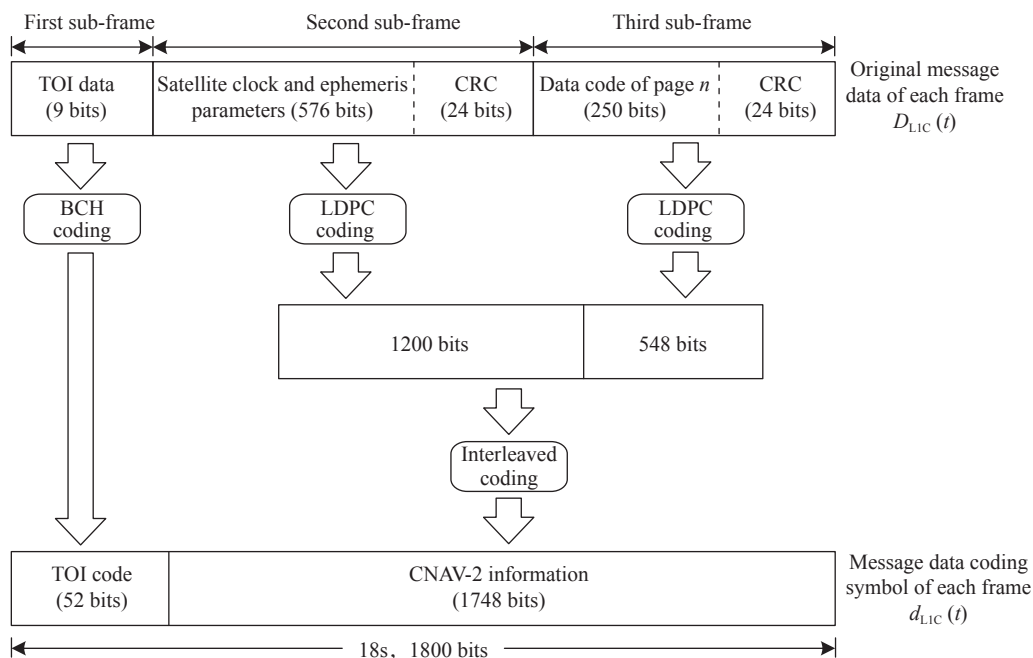


Fig. 1. CNAV-2 message structure and coding.

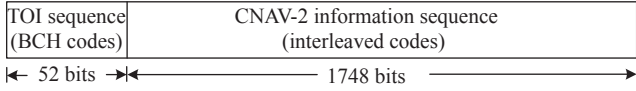


Fig. 2. CNAV-2 message frame structure.

the 52-bit TOI sequence of BCH codes and the 1748-bit information sequence of the interleaved codes. The frame structure is shown in Fig.2.

For the 52-bit data, 2^{52} code words can be obtained by full permutation. However, for the 9-bit TOI sequence, one-to-one relationships are observed between the information bits and the checking bits, and only 2^9 code words can be obtained by using BCH coding. By contrast, for the information sequence of the interleaved codes, no such relationships are observed. Therefore, considering these characteristics of CNAV-2 messages, this paper achieves the frame synchronization of navigation messages by mining the one-to-one relationships in the TOI sequence by using the association rule algorithm.

III. Blind Synchronization Method Based on Association Rules

1. Introduction to association rules

The association rule algorithm is developed by Agrawal and co-workers in order to automatically reveal the hidden association relationship among data items [11]–[17].

$S = \{s_1, s_2, \dots, s_v\}$ represents an itemset. C means task-relevant transaction sets, and each transaction set T constitutes a sub-set of the itemset S . In other words, $T \in S$. For each transaction, there is a unique mapping identifier called TID. For the records of a transaction, if attribute A is in co-existence with attribute B , attribute A is considered to be associated with attribute B . In other words, $A \Rightarrow B$ [18], [19].

Definition 1 The support level of rule $A \Rightarrow B$ in-

dicates the number of occurrences of transactions with attributes $A \cup B$ in the transaction set T .

The support level is considered a useful evaluation indicator. A small value suggests the rare occurrence of the relevant rule. The support level is expressed by the following probability equation:

$$\text{Support}(A \Rightarrow B) = \frac{|\{m : A \cup B \subseteq m, m \in T\}|}{|T|} \quad (1)$$

where m represents data items; and $A \cup B$ represents transactions with attributes A and B .

Definition 2 The confidence level of the rule $A \Rightarrow B$ indicates the percentage share of transactions with attributes A and B in all transactions with attribute A .

The confidence level is considered a determinant of predictability. If the confidence level of a rule is very low, the confident prediction of attribute A from attribute B becomes very difficult. The confidence level is expressed by the following conditional probability equation:

$$\text{Confidence}(A \Rightarrow B) = \frac{|\{m : A \cup B \subseteq m, m \in T\}|}{|\{m : A \subseteq m, m \in T\}|} \quad (2)$$

The symbols in (2) define the same meaning as those in (1).

2. Mining of association attributes of CNAV-2 messages

In the first sub-frame, the 9-bit TOI original message data B is converted into the 52-symbol data D after BCH coding. The coder structure is shown in Fig.3.

For the 9-bit TOI data $B = b_9b_8b_7b_6b_5b_4b_3b_2b_1$, where b_1 represents the least-significant bit, the generation process of code words follows the below steps [6]:

1) The less-significant 8 bits are loaded into the coder from the most significant bit to the least significant

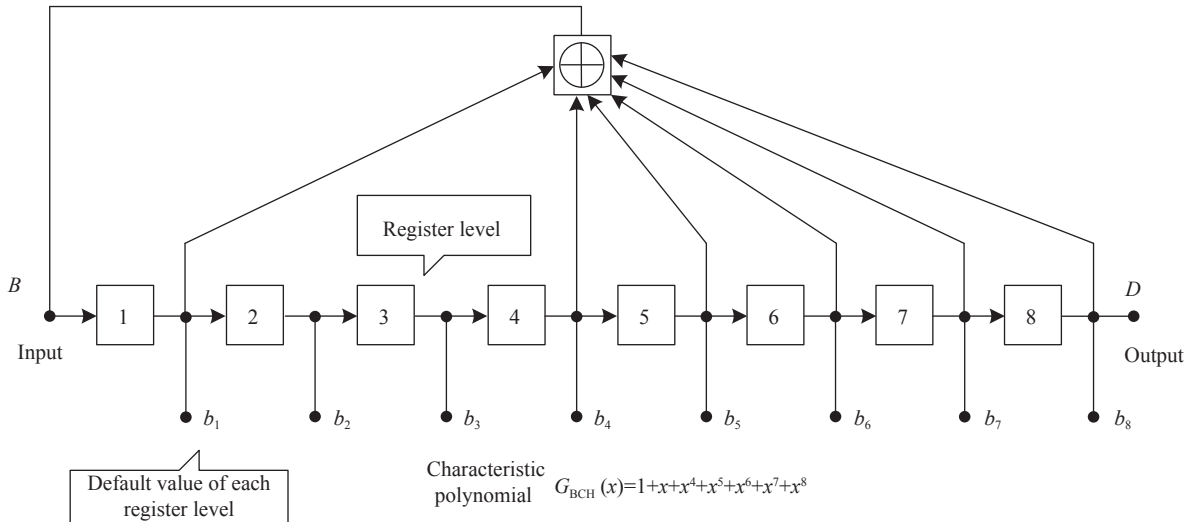


Fig. 3. BCH coder structure.

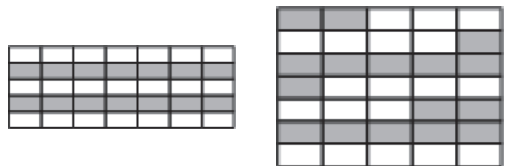
ant bit, and the bit shifting is performed 51 times in order to output 51 codes. The default value of each register level is shown in Fig.3. The value of the last-level register is used as the output code, and the first-output code word is placed at the most-significant bit.

2) Exclusive OR addition is performed for bit b_9 and the above 51 codes one by one.

3) b_9 is placed in front of the code words generated by using exclusive OR addition in order to obtain the 52-bit coding data.

If $D = d_1 d_2 \dots d_{52}$, then $d_1 d_2 \dots d_{52} = b_9(b_{8_1} + b_9) \dots (b_{8_{51}} + b_9)$ (addition modulo 2 is performed in the brackets), where $b_{8_i} (i = 1, 2, \dots, 51)$ is the value of b_8 output by the coder at the instance of i . If $i \leq 8$, then $b_{8_i} = b_{9-i}$; and if $9 \leq i \leq 51$, then $b_{8_i} = b_{8_{i-1}} + b_{8_{i-4}} + b_{8_{i-5}} + b_{8_{i-6}} + b_{8_{i-7}} + b_{8_{i-8}}$. Thus, $b_{8_i} (i = 1, \dots, 51)$ is uniquely determined by B in the 9-bit segment. Considering that $d_j = b_{8_i} + b_9 (9 \leq i \leq 51, j \geq 10)$ and $d_1 d_2 \dots d_9 = b_9(b_{8_1} + b_9) \dots (b_{8_8} + b_9)$, there are one-to-one mapping relationships between code words $d_1 \dots d_9$ and code words $d_{10} \dots d_{52}$.

For a string of received CNAV-2 message data, when the sequence is correctly synchronized, restraint relationships are seen among the BCH code words in subframe 1, and fixed correlation features are shown, as shown in Fig.4 (a). In the absence of the correct sequence synchronization, the restraint relationships among the code words are disturbed, and the mapping relationships are found in a random distribution, as shown in Fig.4(b).



(a) Correct synchronization (b) Incorrect synchronization

Fig. 4. Matrix distribution diagram.

In the example of the (7,3) linear block code, when the code words are found in correct arrangements, the mapping relationships between the information bits and the checking bits are presented in Table 1; and when

$$C = \left[\begin{array}{cccc|ccc} c_i & c_{i+1} & \dots & c_{i+8} & c_{i+9} & \dots & c_{i+51} \\ c_{i+1800} & c_{i+1801} & \dots & c_{i+1808} & c_{i+1809} & \dots & c_{i+1851} \\ \vdots & \vdots & \ddots & \vdots & \vdots & \ddots & \vdots \\ c_{i+(n-1)\cdot 1800} & c_{i+(n-1)\cdot 1800+1} & \dots & c_{i+(n-1)\cdot 1800+8} & c_{i+(n-1)\cdot 1800+9} & \dots & c_{i+(n-1)\cdot 1800+51} \end{array} \right] \quad (3)$$

where $n = \lfloor (L - i + 1) / 1800 \rfloor$. As analyzed above, in the presence of the correct sequence synchronization, the fewest mapping relationships are found in (3); otherwise, more mapping relationships are observed in other cases. Therefore, the sequence that has to be synchronized is divided according to fixed rules in order to ob-

tain the candidate itemset $Q_1\{a_l \rightarrow b_l\} (l = 1, 2, \dots, n)$ (where a_l and b_l represent the decimal numbers for the first 9 bits and the last 43 bits of each row in the matrix C); The grouping is performed for each mapping relationship to obtain the candidate itemset $Q_2\{a_i \rightarrow b_i, x_i\} (i = 1, 2, \dots, j, j \leq n)$, where x_i is the occurrence of

the code words are found in incorrect arrangements, the mapping relationships are presented in Table 2. As shown above, when the code sequence is in correct arrangements, the fewest and fixed mapping relationships are observed; and when the sequence is in incorrect arrangements, the mapping relationships are found in a mess and out of order. In this paper, the mapping relationships are generated between the first 9 code words and the last 43 code words in the BCH coding data of CNAV-2 messages in order to obtain frame synchronization by using association rule mining.

Table 1. Mapping relationships for correct arrangements

Code word	Decimal mapping relationship
[0 0 0 0 0 0 0]	0→0
[0 0 1 1 1 0 1]	1→13
[0 1 0 0 1 1 1]	2→7
[0 1 1 1 0 1 0]	3→10
[1 0 0 1 1 1 0]	4→14
[1 0 1 0 0 1 1]	5→3
[1 1 0 1 0 0 1]	6→9
[1 1 1 0 1 0 0]	7→4

Table 2. Mapping relationships for incorrect arrangements

Code word	Decimal mapping relationship
[0 0 0 1 1 0 1]	0→13
[0 0 1 1 1 0 1]	1→13
⋮	⋮
[0 1 0 0 1 1 1]	2→7
[0 1 1 1 0 1 0]	3→10
[1 0 0 0 1 1 1]	4→7
⋮	⋮
[1 1 1 0 0 1 0]	7→2

3. Algorithm design

Assuming that the length of the CNAV-2 message sequence that has to be synchronized is L , the sequence is divided from the start bit i with a frame length of 1800 bits into $\lfloor (L - i + 1) / 1800 \rfloor$ frames (where $\lfloor \cdot \rfloor$ means rounding down), and the first 52 bits of each frame are arranged to form a matrix, as expressed in (3):

tain the candidate itemset $Q_1\{a_l \rightarrow b_l\} (l = 1, 2, \dots, n)$ (where a_l and b_l represent the decimal numbers for the first 9 bits and the last 43 bits of each row in the matrix C); The grouping is performed for each mapping relationship to obtain the candidate itemset $Q_2\{a_i \rightarrow b_i, x_i\} (i = 1, 2, \dots, j, j \leq n)$, where x_i is the occurrence of

each mapping relationship. Then, the screening is conducted to determine the mapping relationships in Q_2 with the minimum support s ; and the mapping relationships $a_i \rightarrow b_i$ with $x_i < s$ are deleted from the candidate Q_2 to obtain the candidate itemset $Q_3\{a_m \rightarrow b_m\}$ ($m = 1, 2, \dots, z, z \leq j$). Finally, the confidence t of Q_3 is calculated for Q_2 according to (4):

$$\text{Confidence}(Q_3/Q_1) = \frac{z}{l} \quad (4)$$

In the presence of the correct sequence synchronization, the fewest mapping relationships are observed, and the highest confidence is achieved. Thus, the correct frame synchronization can be achieved.

4. Computational complexity analysis

The proposed method's computational complexity is reflected in two major aspects: first, the conversion of binary sequence into decimal numerals, and second, the computation of confidence value. If the length of the sequence to be synchronized is L , then there are $\lfloor L/1800 \rfloor$ rows in the matrix established by dividing the code sequence according to the fixed rules. Considering that two-segment division is conducted, the computational complexity is $2 \lfloor L/1800 \rfloor$ during each conversion of binary sequence to decimal numerals; and assuming that

$$\begin{aligned} c_1 c_2 \dots c_L \rightarrow C'_1 &= \begin{bmatrix} c_1 & c_2 & \dots & c_{1800} \\ c_{1801} & c_{1802} & \dots & c_{3600} \\ \vdots & \vdots & \ddots & \vdots \\ c_{(\lfloor L/1800 \rfloor - 1) \cdot 1800 + 1} & c_{(\lfloor L/1800 \rfloor - 1) \cdot 1800 + 2} & \dots & c_{(\lfloor L/1800 \rfloor) \cdot 1800} \end{bmatrix} \\ \rightarrow C_1 &= \begin{bmatrix} c_1 & c_2 & \dots & c_{52} \\ c_{1801} & c_{1802} & \dots & c_{1852} \\ \vdots & \vdots & \ddots & \vdots \\ c_{(\lfloor L/1800 \rfloor - 1) \cdot 1800 + 1} & c_{(\lfloor L/1800 \rfloor - 1) \cdot 1800 + 2} & \dots & c_{(\lfloor L/1800 \rfloor - 1) \cdot 1800 + 52} \end{bmatrix} \end{aligned} \quad (5)$$

Step 2: The matrix C_i is divided by using the bisection method, and the first 9 bits and the last 43 bits are separately converted into decimal numbers in order to obtain the mapping relationship itemset T_i . The mapping relationships N_i of the itemset T_i are counted,

$$\begin{aligned} C_1 &= \left[\begin{array}{ccc|ccc} c_1 & \dots & c_9 & c_{10} & \dots & c_{52} \\ c_{1801} & \dots & c_{1809} & c_{1810} & \dots & c_{1852} \\ \vdots & \ddots & \vdots & \vdots & \ddots & \vdots \\ c_{(\lfloor L/1800 \rfloor - 1) \cdot 1800 + 1} & \dots & c_{(\lfloor L/1800 \rfloor - 1) \cdot 1800 + 9} & c_{(\lfloor L/1800 \rfloor - 1) \cdot 1800 + 10} & \dots & c_{(\lfloor L/1800 \rfloor - 1) \cdot 1800 + 52} \end{array} \right] \\ \rightarrow T_1 &= \left[\begin{array}{cc|c} a_1 & \rightarrow & b_1 \\ a_2 & \rightarrow & b_2 \\ \vdots & \ddots & \vdots \\ a_{\lfloor L/1800 \rfloor} & \rightarrow & b_{\lfloor L/1800 \rfloor} \end{array} \right] \end{aligned} \quad (6)$$

Step 3: The traversal method is adopted for the start bit i . The above process is repeated to count the mapping relationships $N_i (i = 1, 2, \dots)$ and calculate the confidence level t_i of each itemset T_i .

there are K mapping relationships with minimum support, and H occurrences of each mapping relationship on average, the computational complexity is $K(1+H)$ for the computation of confidence value each time. For the frame synchronization process with traversal search for i start bits, the total computational complexity is $i \cdot [2 \lfloor L/1800 \rfloor + K(1+H)]$. In view of the small values of K and H in the proposed method, the parts with low computational complexity are ignored; and thus the computational complexity is $O(2i \lfloor L/1800 \rfloor)$ for the proposed method.

5. Algorithm steps

In the absence of the correct synchronization of message data, the mapping relationships are found in a random distribution, and the number of occurrences of each mapping relationship is estimated as 1. Therefore, the mapping relationship confidence level t is calculated assuming the minimum support $s = 2$. The below algorithm steps are followed.

Step 1: Assuming that the length of the received message data is L , the data is divided from the start bit $i (i = 1, 2, \dots, 1800)$ with a row length of 1800 bits in order to obtain the matrix C'_i , and the first 52 columns of the matrix C'_i are arranged in order to obtain the matrix C_i according to (5).

and the mapping relationship confidence level t_i of the itemset T_i is calculated with the support level higher than or equal to the minimum support $s = 2$. In (6), $a_{\lfloor L/1800 \rfloor}$ and $b_{\lfloor L/1800 \rfloor}$ are decimal numerals for the first 9 bits and last 43 bits in each row of matrix C_1 .

Step 4: A comparative analysis is performed for the mapping relationships $N_i (i = 1, 2, \dots)$ and the confidence levels t_i of various start bits i . The correct synchronization bit is the start bit associated with the fewest

mapping relationships and the highest confidence level.

IV. Simulation Testing

Test 1 Frame synchronization in the absence of the code error

When there were no code errors, CNAV-2 message data was simulated whose length was 9000010 bits and the correct start bit was bit 11. The code sequence was divided from the first bit with a row length of 1800 bits in order to obtain the 5000×1800 matrix C'_1 . The first 52 columns of the matrix C'_1 were arranged to form the matrix C_1 , and the first 9 bits and the last 43 bits of each row of the matrix C_1 were separately converted into decimal numbers to count the mapping relationships N_1 and calculate the confidence level t_1 of the mapping relationship itemset T_1 . Then, the start bit was shifted backward bit by bit, and this process was repeated in order to obtain the distribution of the mapping relationships and their confidence levels, as shown in Figs.5 and 6.

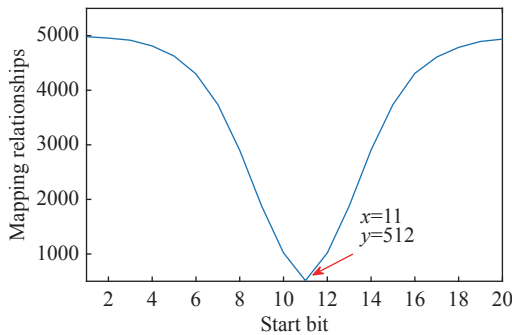


Fig. 5. Distribution diagram of mapping relationships.

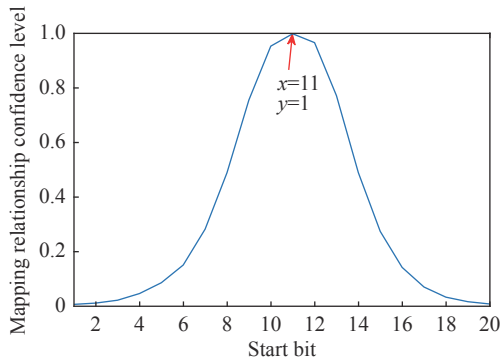


Fig. 6. Distribution diagram of the mapping relationship confidence level.

As shown in Figs.5 and 6, when the start bit is bit 11, in this case, a total of 512 mapping relationships are observed, which are much fewer than those in other cases; and the confidence level is at the maximum and equal to 1. Therefore, the correct synchronization bit of the message data is bit 11. In this case, the correct synchronization is achieved.

When there were no code errors, CNAV-2 message data was simulated whose length was 9000010 bits and

the correct start bit was bit 4. Other conditions remain unchanged. This process was repeated in order to obtain the distribution of the mapping relationships and their confidence levels, as shown in Figs.7 and 8.

As shown in Figs.7 and 8, when the start bit is bit 4, in this case, a total of 512 mapping relationships are observed, which are much fewer than those in other cases; and the confidence level is at the maximum and equal to 1. Therefore, the correct synchronization bit of the message data is bit 4. In this case, the correct synchronization is achieved.

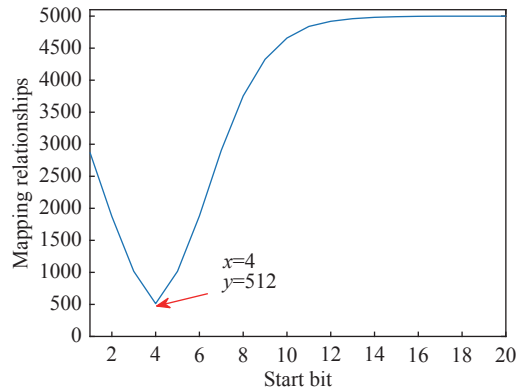


Fig. 7. Distribution diagram of mapping relationships.

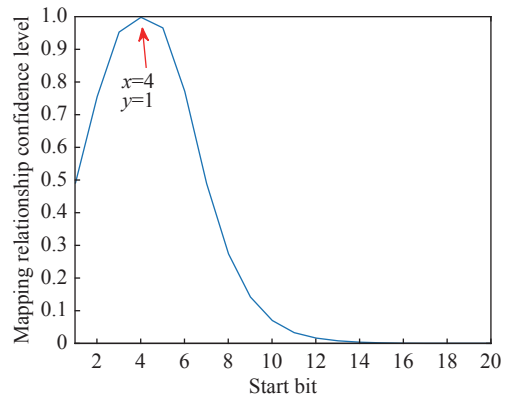


Fig. 8. Distribution diagram of the mapping relationship confidence level.

Test 2 Performance analysis in the presence of the code error

When the code error rate was 1%, CNAV-2 message data was simulated whose length was 9000010 bits, and the start bit was bit 11. This test process was repeated in order to obtain the distribution of the mapping relationships and their confidence levels, as shown in Figs.9 and 10.

As shown in Figs.9 and 10, when the bit error rate is 1%, and the start bit is bit 11, in this case substantially more mapping relationships are observed, but they are still fewer than those in other cases; and the confidence level is substantially lower than the confidence level when there are no code errors, but it is still higher than that in other cases. Therefore, the correct

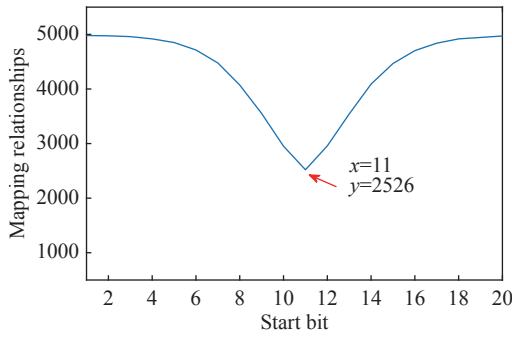


Fig. 9. Distribution diagram of mapping relationships.

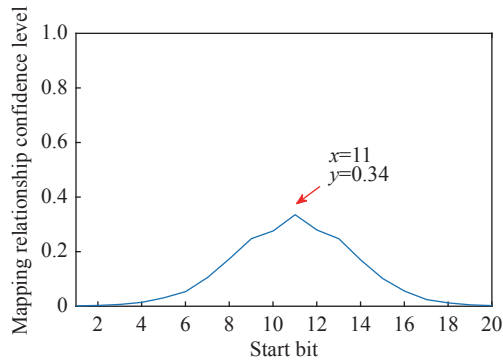


Fig. 10. Distribution diagram of the mapping relationship confidence level.

synchronization bit of the message data is bit 11. In this case, the correct synchronization is achieved.

Then, the code error rate was increased to 5%, and this test process was repeated in order to obtain the distribution of the mapping relationships and their confidence levels, as shown in Figs.11 and 12.

As shown in Figs.11 and 12, when the code error rate is 5%, and the start bit is bit 11, in this case, the mapping relationships are similar to but still fewer than those in other cases; and the confidence level is similar to but still higher than that in other cases. In this case, the correct synchronization can be achieved.

Then, the code error rate was increased to 8% and the correct start bit was bit 4. This test process was repeated in order to obtain the distribution of the mapping relationships and their confidence levels, as shown in Figs.13 and 14.

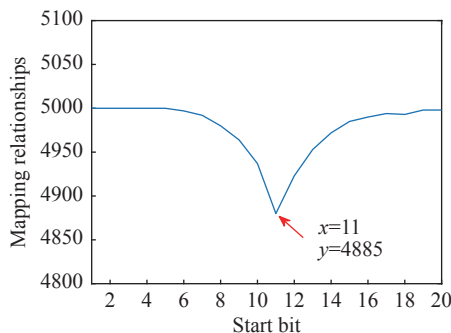


Fig. 11. Distribution diagram of mapping relationships.

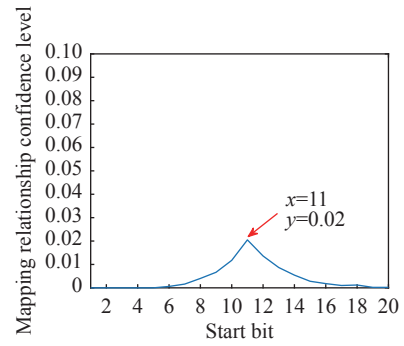


Fig. 12. Distribution diagram of the mapping relationship confidence level.

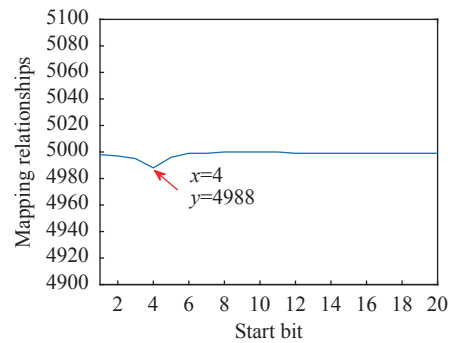


Fig. 13. Distribution diagram of mapping relationships.

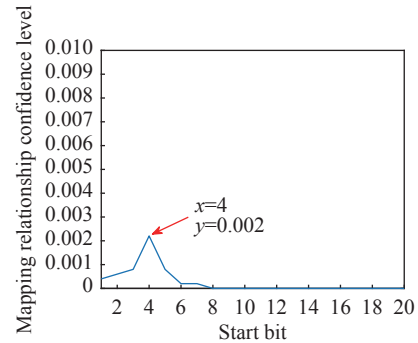


Fig. 14. Distribution diagram of the mapping relationship confidence level.

As shown in Figs.13 and 14, when the code error rate is 8%, and the start bit is bit 4, in this case, the mapping relationships are fewer than those in other cases and the confidence level is higher than that in other cases. In this case, the correct synchronization can be achieved.

Test 3 Algorithm performance comparison

The proposed algorithm was evaluated in comparison to the sliding window algorithm described in [6]. The Monte Carlo simulation testing was performed 100 times for CNAV-2 message data with a length of 9000010 bits and a start bit location of the 11th bit, with code error rates ranging from 0.01 to 0.09. Fig.15 depicts the test results.

As shown in Fig.15, the probability of accurate synchronization was close to 100 percent for the apriori algorithm and around 97 percent for the sliding win-

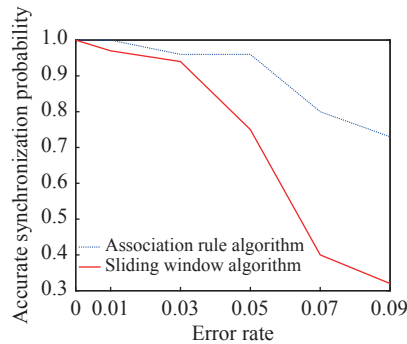


Fig. 15. Performance comparison.

sliding window algorithm with a code error rate of 1%. Meanwhile, for code error rates greater than 7%, the probability of accurate synchronization was greater than 70% for the apriori algorithm and less than 40% for the sliding window algorithm.

V. Conclusions

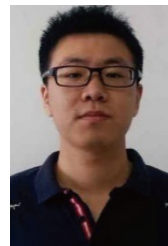
This paper discusses the frame synchronization of CNAV-2 messages in GPS L1C signals and proposes a frame synchronization algorithm based on association rules. It provides a new way of thinking about frame synchronization. By configuring the value of minimum support, the number of candidate item-sets was greatly reduced, improving the computational efficiency of the proposed algorithm. On the basis of type analysis of mapping relations and value determination of confidence level, the proposed algorithm was found to outperform the existing algorithm in terms of error performance. The proposed algorithm achieves correct synchronization by traversing the start bit. The computational complexity of massive data increases, as does the system performance requirement.

References

- [1] J. Zhang, C. Shao, and Y. Hou, "Optimal quantification method for LDPC code decoding of GPS L1C signal," *Science of Surveying and Mapping*, vol.44, no.1, pp.32–35, 2019.
- [2] K. Ghorbani, N. Orouji, M. R. Mosavi, "Navigation message authentication based on one-way Hash chain to mitigate spoofing attacks for GPS L1," *Wireless Personal Communications*, vol.113, no.6, pp.1743–1754, 2020.
- [3] G. Wang, "Frame synchronization technique for GPS SBAS L1 signal," *Modern Navigation*, vol.10, no.4, pp.241–246, 2019.
- [4] X. Fang, H. Peng, and L. Wu, "A quick frame synchronization method for navigation message based on ephemeris matching," *Modern Radar*, vol.43, no.4, pp.34–38, 2021.
- [5] C. Wang, L. ZHANG, C. ZHENG, *et al.* "Research on phase optimal matching strategy of GPS L1C signal coverage code," in *Proc. of the 6th China Satellite Navigation Academic Annual Conference*, Xi'an, China, pp.1–5, 2015.
- [6] G. Xie, *Principle of Global Navigation Satellite System*, Beijing: Publishing House of Electronics Industry, pp.143–158, 2013.
- [7] Z. Li and J. Huang, *GPS Surveying and Data Processing*,

Wuhan: Wuhan University Press, pp.15–53, 2005.

- [8] Q. Li, "Study on the method and performance of fast frame synchronization of GPS L1C navigation message," in *Proc. of China Satellite Navigation Academic Annual Conference*, Xi'an, China, pp.1–5, 2015.
- [9] T. South and Y. Kou, "Implementation and performance analysis of soft decision decoding for CNAV-2 messages," *Journal of Time and Frequency*, vol.38, no.2, pp.112–113, 2015.
- [10] Z. Deng, J. Li, C. Li, *et al.*, "Characteristic analysis and fast adaptive synchronization algorithm of GPS CNAV-2 navigation message synchronization code," in *Proc. of China Satellite Navigation Conference*, Nanjing, China, pp.32–38, 2014.
- [11] L. Liu, J. Wen, Z. Zheng, *et al.*, "An improved approach for mining association rules in parallel using spark streaming," *Int J Circ Theor Appl*, vol.49, no.4, pp.1028–1039, 2021.
- [12] A. Mehta and D. Bura, "Mining of association rules in R using apriori algorithm," in *Advances in Communication and Computational Technology, Lecture Notes in Electrical Engineering (vol.668)*, Springer, Singapore, pp.14–25, 2021.
- [13] Yüksel Akay nvan, "Market basket analysis with association rules," *Communication in Statistics-Theory and Methods*, vol.50, no.7, pp.1615–1628, 2021.
- [14] Z. Zhao , Z. Jian , G. Gaba, *et al.*, "An improved association rule mining algorithm for large data," *Journal of Intelligent Systems*, vol.30, no.1, pp.750–762, 2021.
- [15] K. Shimada, T. Arahira, and T. Hanioka, "Association rule-based classifier using artificial missing values," in *Advances in Data Mining, Applications and Theoretical Aspects – ICDM 2017, Lecture Notes in Computer Science (vol.0357)*, Springer, Cham, pp.57–67, 2017.
- [16] Z. Li, F. Yu, and H. Zhang, "A fast algorithm for mining temporal association rules based on a new definition," in *Proc. of 2017 13th International Conference on Natural Computation, Fuzzy Systems and Knowledge Discovery (ICNC-FSKD)*, Guilin, China, pp.1548–1553, 2017.
- [17] P. Bemarisika and A. Totohasina, "An efficient method for mining informative association rules in knowledge extraction," in *Machine Learning and Knowledge Extraction – CD-MAKE 2020, Lecture Notes in Computer Science (vol.12279)*, Springer, Cham, pp.227–247, 2020.
- [18] C. Hui and L. Jiao, "Mining frequent itemsets of novel characters based on association rules," *Journal of Physics: Conference Series*, vol.1550, article no.032158, 2020.
- [19] G. Jie, "Research on application of improved association rules mining algorithm in personalized recommendation," *Journal of Physics: Conference Series*, vol.1744, article no.032111, 2021.



LI Xinhao was born in 1989. He received the Ph.D. degree in communication and information systems from Electronic Engineering Institute in 2017. His research interests include blind recognition of channel coding and blind recognition of frame structure.
(Email: lixinhao1989616@126.com)

MA Tao was born in 1979. He received the Ph.D. degree in information processing from Electronic Engineering Institute in 2009. His research interests include modeling and simulation in cyberspace. (Email: matao7926@163.com)

QIAN Qishu was born in 1995. She received the M.S. degree in optical engineering from National University of Defense Technology in 2019. Her research interests include target tracking. (Email: creamy777@163.com)